Nature Methods

A genome-scale shRNA resource for transgenic RNAi in *Drosophila*

Jian-Quan Ni, Rui Zhou, Benjamin Czech, Lu-Ping Liu, Laura Holderbaum, Donghui Yang-Zhou, Hye-Seok Shim, Dominik Handler, Phillip Karpowicz, Richard Binari, Matthew Booker, Julius Brennecke, Lizabeth A Perkins, Gregory J Hannon & Norbert Perrimon

Supplementary Figure 1	Vectors tested for efficient expression in the female germline.
Supplementary Figure 2	VALIUM20 and VALIUM22 are *miR-1* based shRNA vectors for transgenic RNAi.
Supplementary Figure 3	VALIUM20 is a very effective vector for somatic RNAi.
Supplementary Figure 4	Leaky expression by VALIUM20-shRNA transgenes.
Supplementary Figure 5	Biogenesis of shRNAs and their loading into effector complexes.
Supplementary Figure 6	Abundance and processing accuracy of shRNAs.
Supplementary Figure 7	VALIUM11 and VALIUM12 vectors are not as effective as VALIUM10 to generate somatic phenotypes.
Supplementary Figure 8	Dependence of shRNA-mediated knockdowns on mother age.
Supplementary Table 1	Analysis of oogenesis phenotypes using shRNA lines in VALIUM20.
Supplementary Table 2	ShRNA lines targeting genes that are not required for viability.
Supplementary Table 3	Transgenic long-hairpin RNAi lines analyzed for oogenesis phenotypes.
Supplementary Note 1	Additional text
Supplementary Note 2	Vectors construction
Supplementary Note 3	Primer sequences

TABLES AND FIGURES

Supplementary Figure 1: Vectors tested for efficient expression in the female germline.

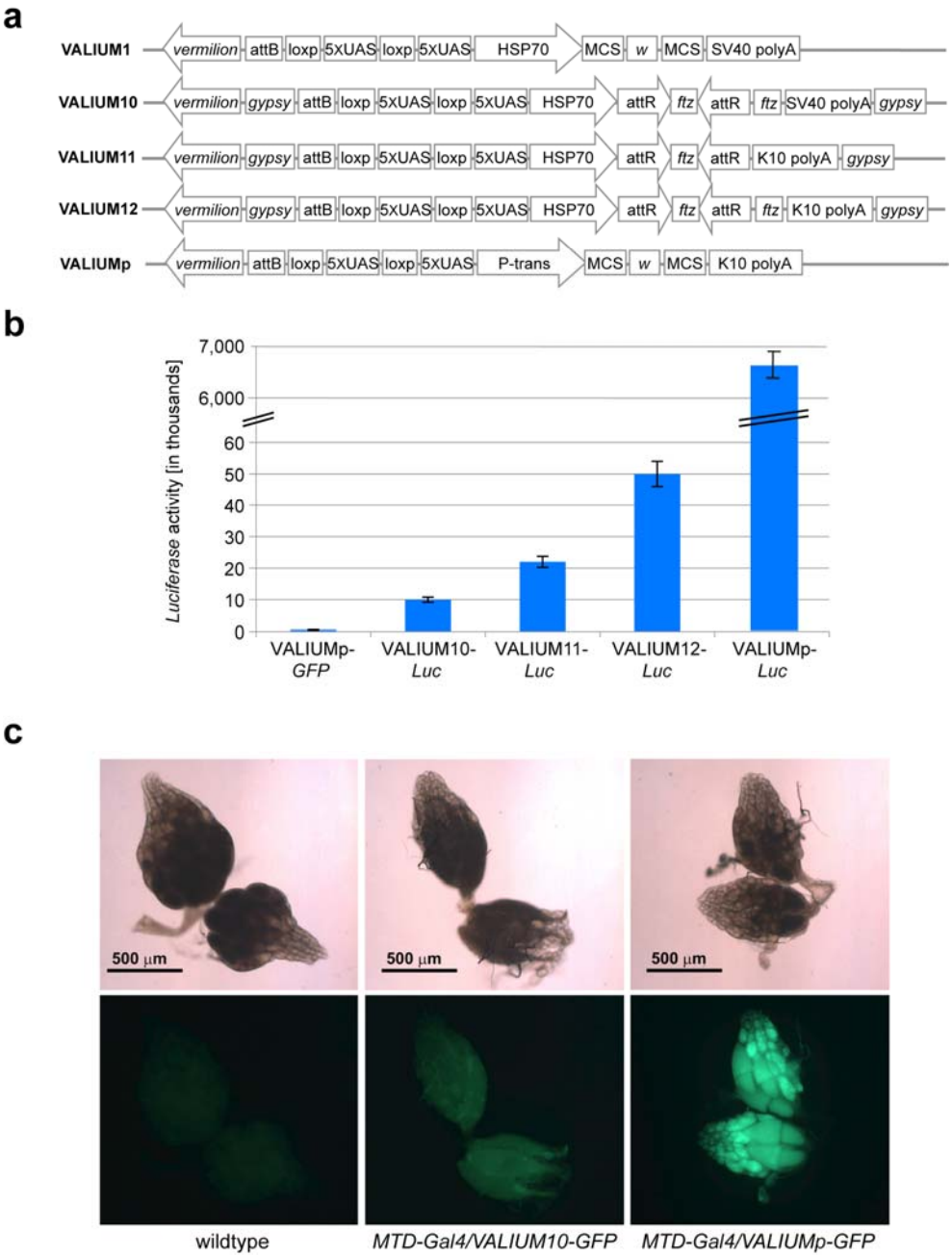

a. Structure of the VALIUM vectors tested for germline expression and their abilities to generate oogenesis and maternal effect phenotypes.

b. *Luciferase* expression levels in the indicated *MTD-Gal4* driven *VALIUM-Luciferase* flies.

c. Expression of *GFP* in *MTD-Gal4/VALIUM10-GFP* and *MTD-Gal4/VALIUMp-GFP*. None of these vectors generated phenotypes during oogenesis and embryogenesis with the

Nature Methods: doi.10.1038/nmeth.1592

lines tested (Supplementary Table 3).

Supplementary Figure 2: VALIUM20 and VALIUM22 are *miR-1* based shRNA vectors for transgenic RNAi.

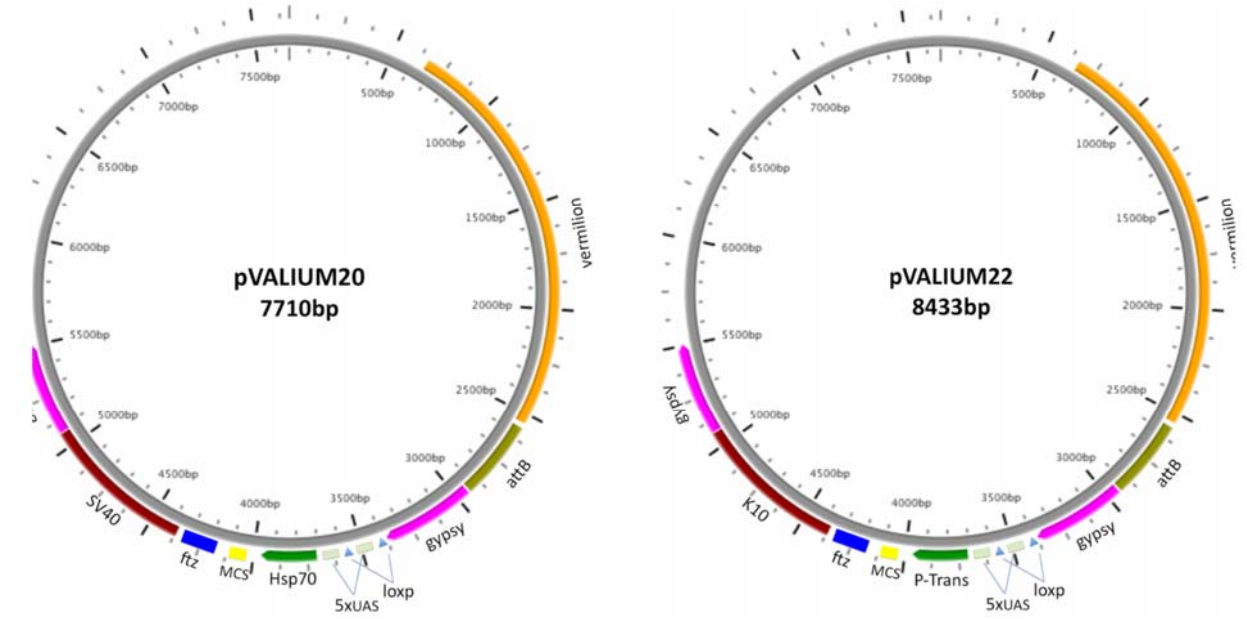

VALIUM20 contains *vermilion* as a selectable marker, an attB sequence to allow for targeted, phiC31-mediated integration at genomic attP landing sites, two pentamers of UAS (one can be excised using the Cre/loxP system to generate a 5XUAS derivative), the *hsp70* core promoter; the an SV40 polyadenylation signal, and an intronic sequence to facilitate RNA nuclear export. The relevant sequences are flanked by two gypsy insulators to ensure stable transgene expression. VALIUM22 comprises essentially the same features except that it contains the K10 3'UTR and the P-element transposase minimal promoter.

Nature Methods: doi.10.1038/nmeth.1592

Supplementary Figure 3: VALIUM20 is a very effective vector for somatic RNAi.

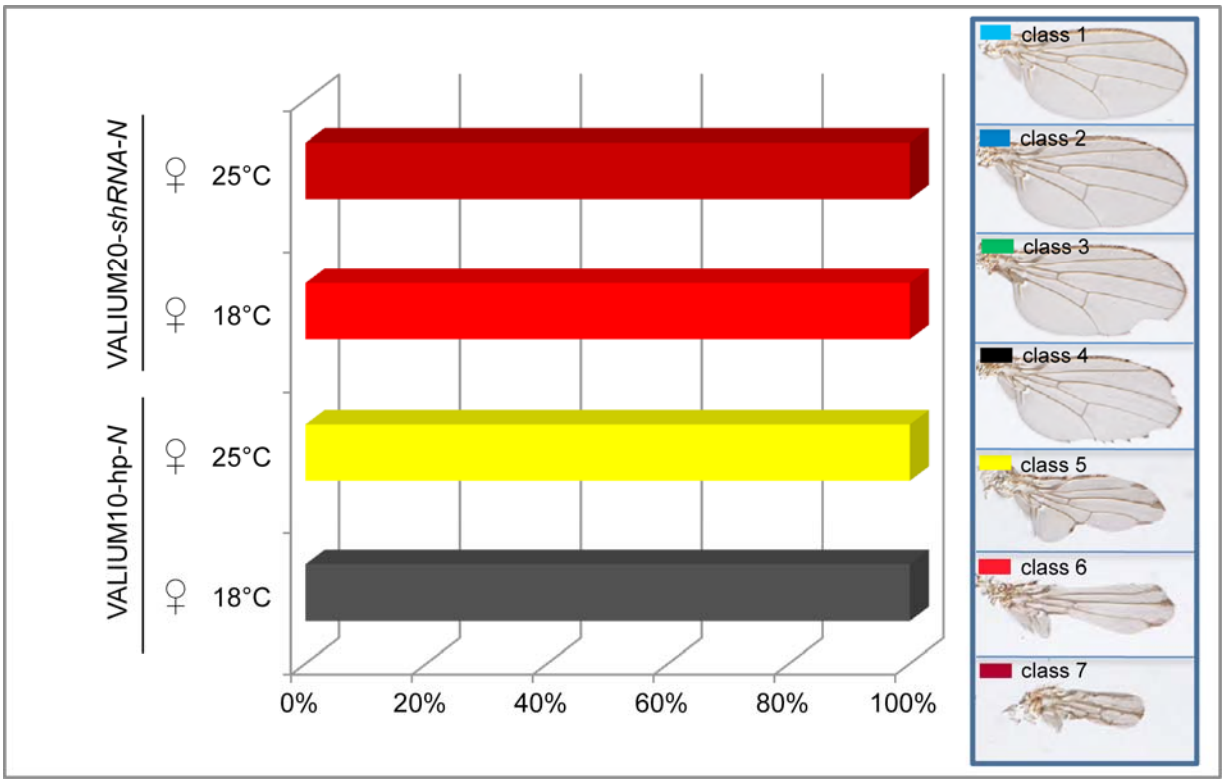

The phenotypes of N knockdown using long-hairpins (VALIUM10) and shRNAs (VALIUM20) are compared in the wing. *C96-Gal4* was used to express *VALIUM10-hp-N* or *C96-Gal4/VALIUM20-shRNA-N***.** Phenotypes were classified by the severity of their wing defects[1] (class 1: wildtype or a few bristles missing; class 2: margin bristles missing but no notches; class 3: Moderate wing notching; class 4: extensive wing notching; class 5: most of the wing margin is missing; class 6: complete lack of wing margin and the wing blade is greatly reduced in size; class 7: Wings are almost completely missing. Note that wing images labeled as “class 1” and “class 7” are also presented in **Fig. 1d**).

Nature Methods: doi.10.1038/nmeth.1592

Supplementary Figure 4: Leaky expression by VALIUM20-shRNA transgenes.

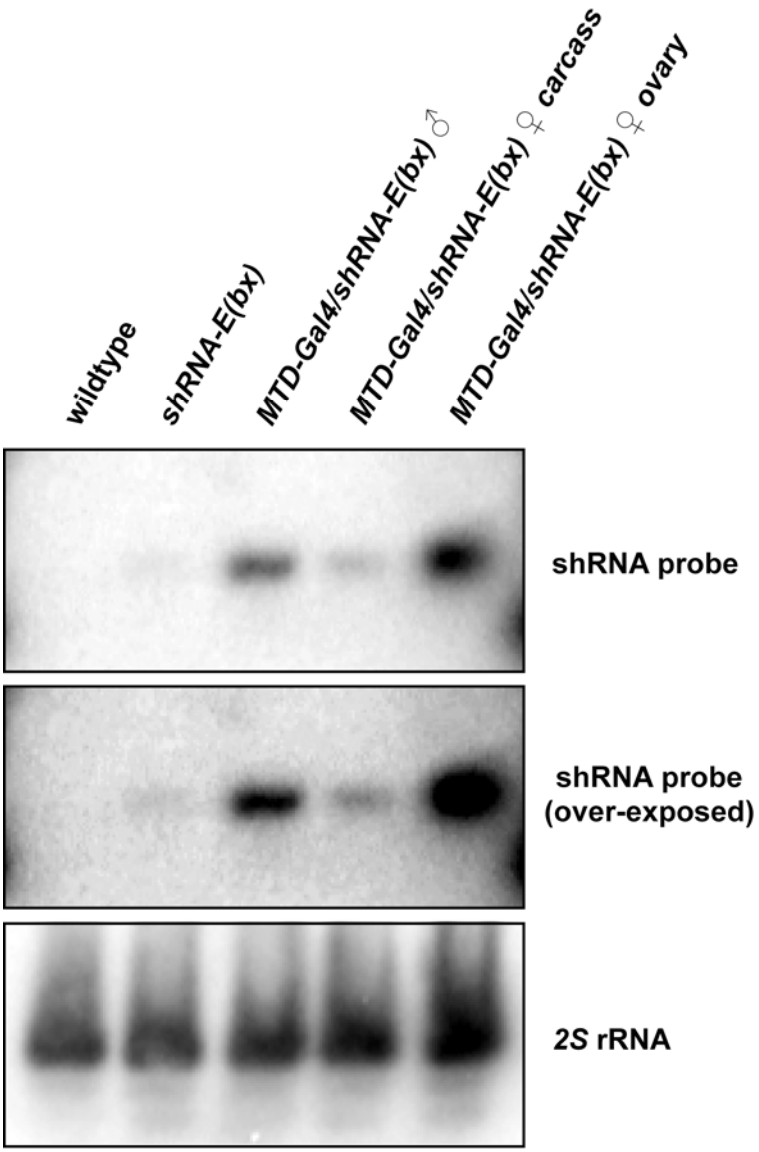

Northern blotting showing the expression levels of *MTD-Gal4/UAS-shRNA-E(bx)* in total RNA preparation from (left to right) wildtype flies, *MTD-Gal4/UAS-shRNA-E(bx)* parental stocks, *MTD-Gal4/UAS-shRNA-E(bx)* males, carcasses of *MTD-Gal4/UAS-shRNA-E(bx)* females in which ovaries have been removed, or ovaries of *MTD-Gal4/UAS-shRNA-E(bx)* females. An over-exposed image is shown in the middle panel. *2S* rRNA serves as loading control.

Nature Methods: doi.10.1038/nmeth.1592

Supplementary Figure 5: Biogenesis of shRNAs and their loading into effector complexes.

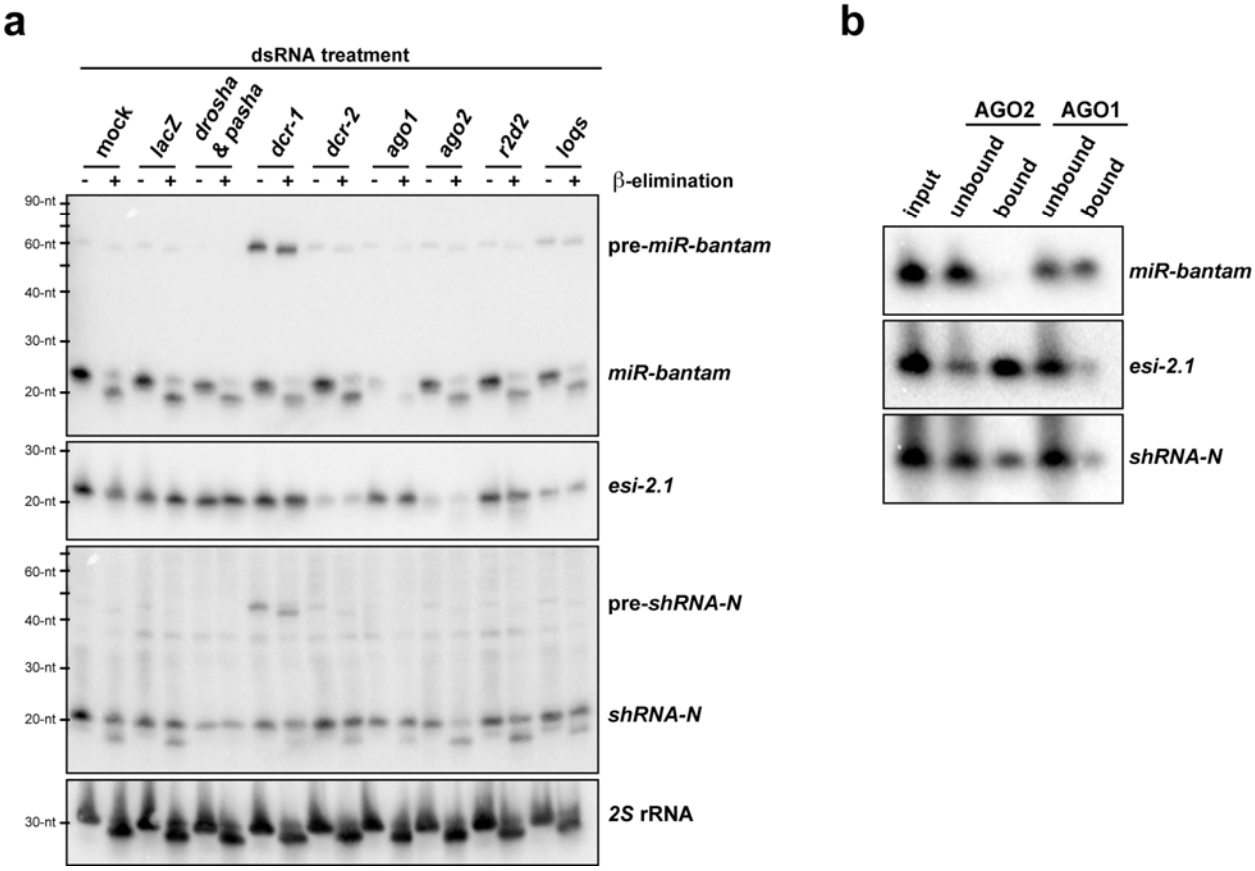

a. Northern blotting showing the steady-state levels of a representative shRNA (*shRNA-N* in VALIUM20) as well as those of an endogenous siRNA (*esi-2.1*) and miRNA (*miR-bantam*) in cultured *Drosophila* cells upon dsRNA-mediated depletion of canonical components of the siRNA and miRNA pathways (knockdowns indicated). In addition, a fraction of the RNA samples was subjected to periodate treatment followed by β-elimination (indicated by +/-). *2S* rRNA serves as the loading control.

b. Cytoplasmic extracts from cells expressing the same shRNA and Flag-tagged-AGO2 were evenly split and subjected to immunoprecipitation using anti-AGO1 and anti-Flag antibodies, respectively. Total RNAs recovered from the immunoprecipitates, as well as those recovered from cell extracts prior to and after immunoprecipitation, were subjected to sequential Northern blotting using probes against *esi-2.1*, *miR-bantam* and *shRNA-N*.

Nature Methods: doi.10.1038/nmeth.1592

Supplementary Figure 6: Abundance and processing accuracy of shRNAs.

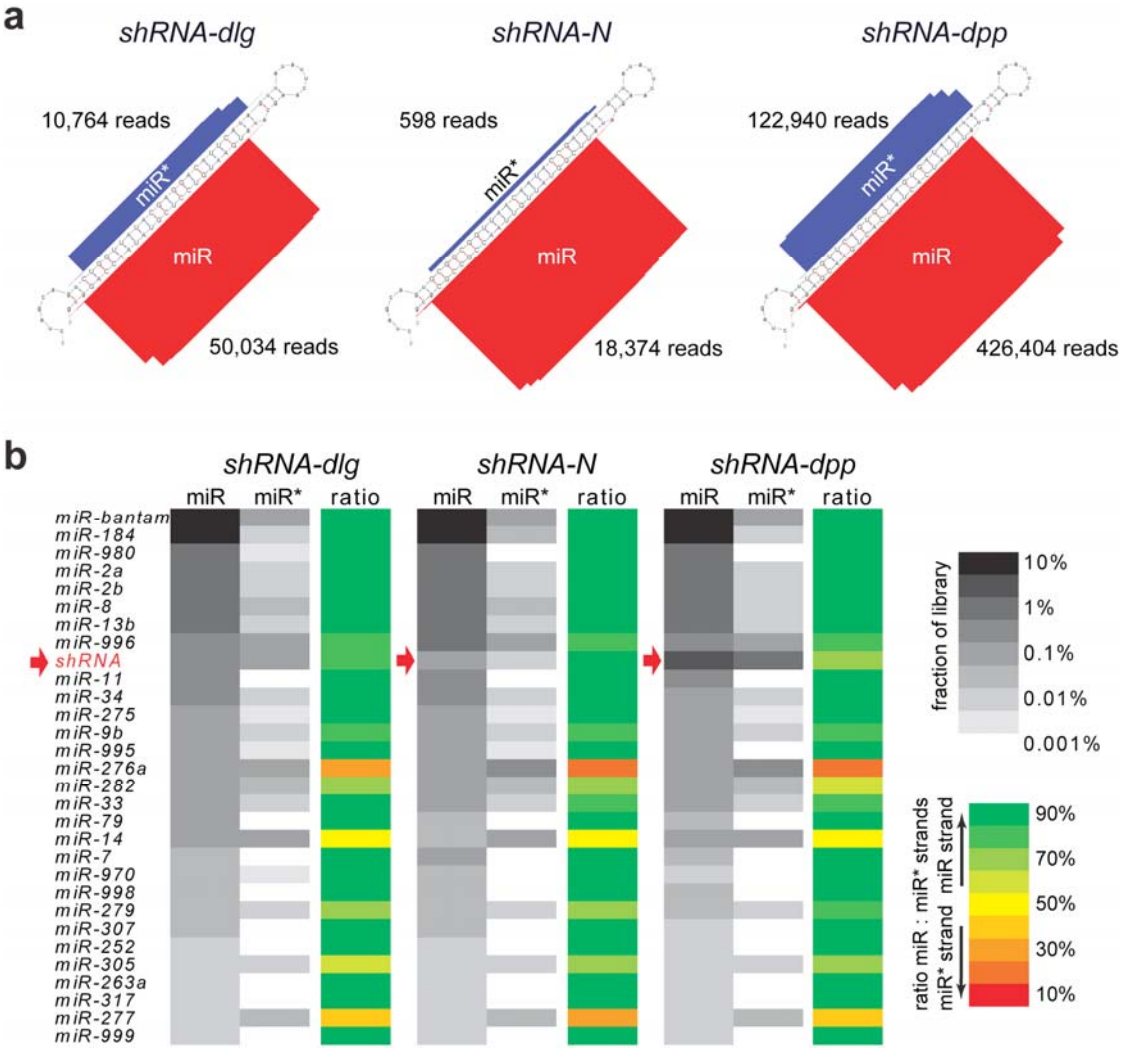

a. Cultured *Drosophila* cells were independently transfected with three different shRNAs and small RNAs were sequenced. Display of the shRNA precursors together with normalized cloning counts in each of the indicated small RNA libraries. Abundances of guide/miR strands (shown in red) and passenger/miR* strands (shown in blue) are indicated by bars. The accuracy of 5' end processing for the shown shRNAs is represented by sharp peaks at the intended sites.

b. Heat maps showing relative levels of the 30 most abundant microRNAs and the indicated shRNA (highlighted by the arrow) in each small RNA library. Both, miR and miR* strands are indicated separately in grey scale, while the ratio between miR and miR* strands is shown in green-red scale.

Nature Methods: doi.10.1038/nmeth.1592

Supplementary Figure 7: **VALIUM11 and VALIUM12 vectors are not as effective as VALIUM10 to generate somatic phenotypes.**

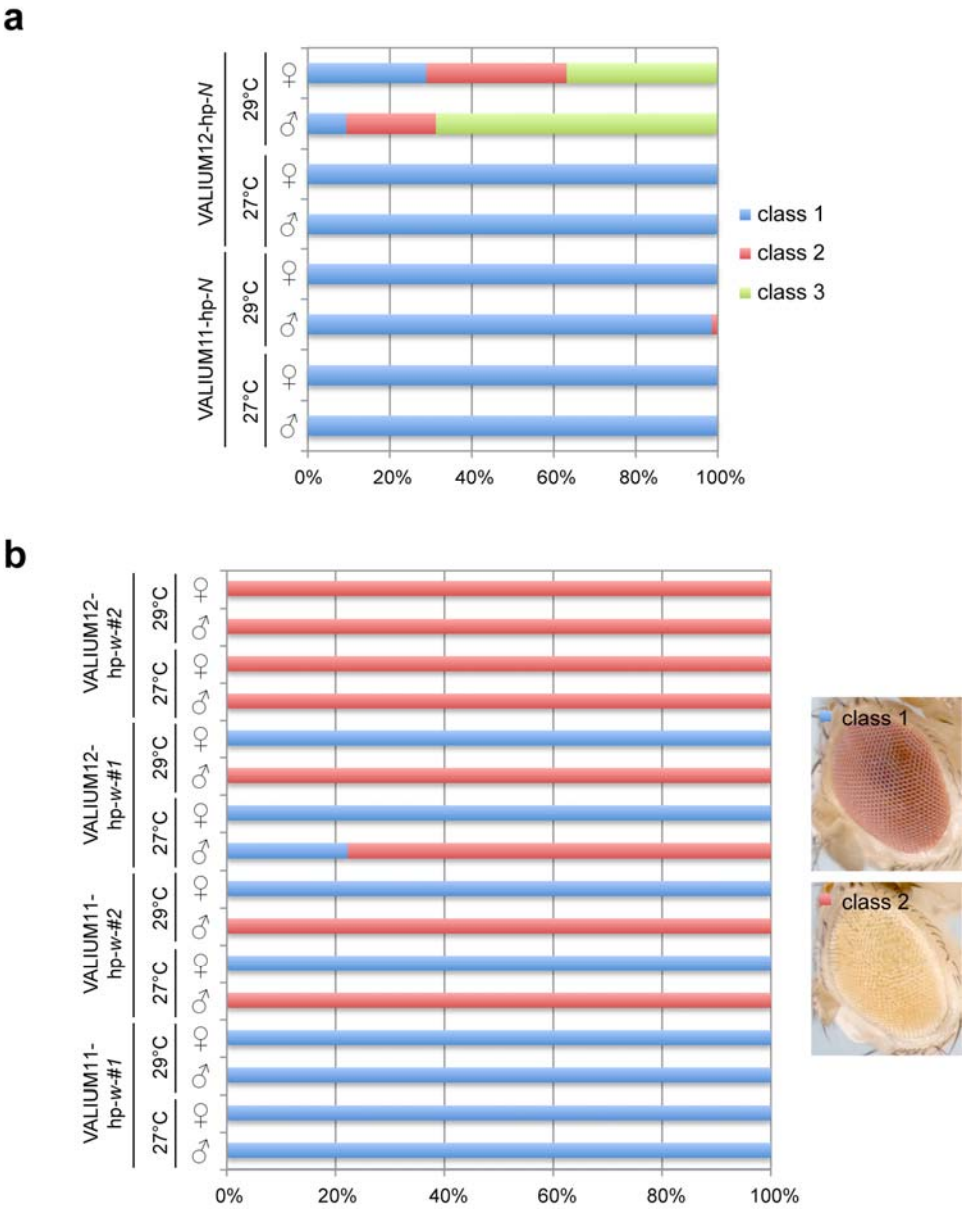

a. *C96-Gal4/VALIUM11-hp-N* and *C96-Gal4/VALIUM12-hp-N* were tested for their wing phenotypes. Phenotypes were classified by the severity of their wing defects (class 1: wildtype or a few bristles missing; class 2: margin bristles missing but no notches; and class 3: moderate wing notching. More details on classification can be found in Supplementary Fig. 3). The phenotypes were analyzed in males and females and at different temperatures.

b. Two different shRNAs against *white* were tested in either VALIUM11 or VALIUM12. For expression, eye-specific *GMR-Gal4* was used.

Nature Methods: doi.10.1038/nmeth.1592

Supplementary Figure 8: Dependence of shRNA-mediated knockdowns on mother age.

a

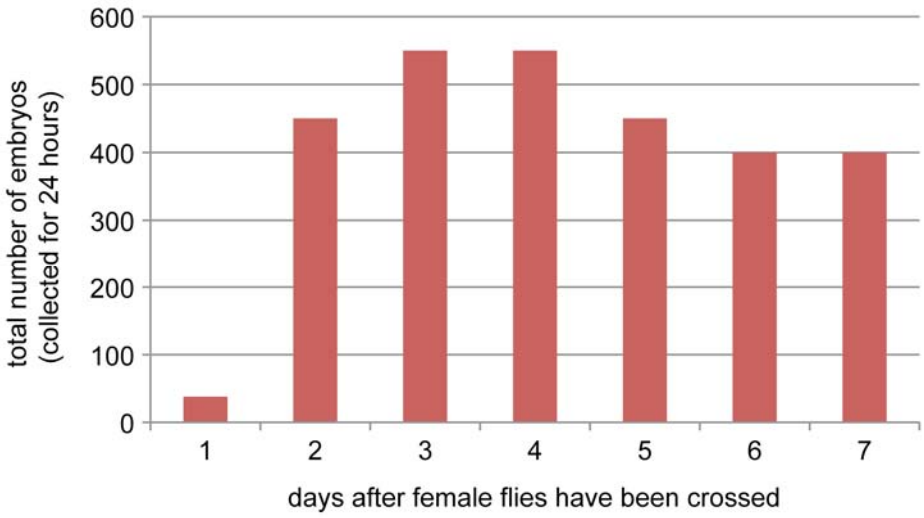

b

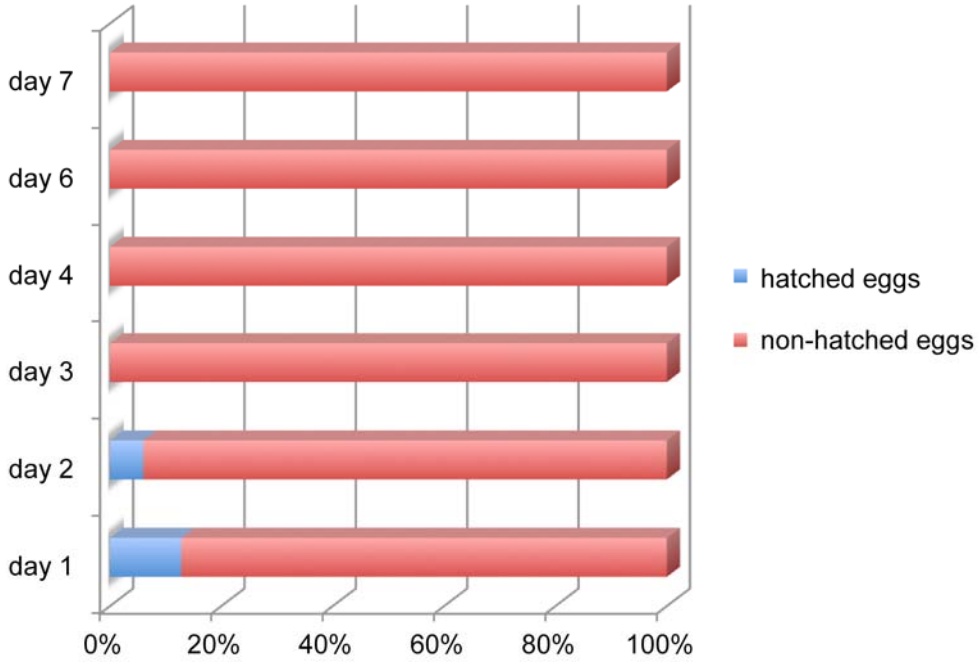

Age dependence of the neurogenic phenotypes in eggs derived from *MTD-Gal4/VALIUM20-shRNA-N* mothers crossed to siblings. The number of eggs collected at different days (**a**) and the percentage of eggs hatching (**b**) are indicated.

Nature Methods: doi.10.1038/nmeth.1592

Supplementary Table 1: Analysis of oogenesis phenotypes using shRNA lines in VALIUM20.

Genes	Temperature	Hairpin ID	Fertility Phenotype	Ovaries	*HeT-A*	*Blood*
w		SH00017.N	lots of eggs and larvae	normal	1	1
spn-E	29C	SH00574.N	lots of eggs, no larvae	normal	69.13	160.35
	29C				39.40	79.59
	29C				107.79	177.13
	29C				114.19	155.21
	25C		lots of eggs, no larvae	normal	53.19	199.99
	25C				53.61	186.12
	25C				56.43	239.14
AGO3	29C	SH00108.N	lots of eggs, few larvae	normal	23.95	160.88
	29C				15.47	127.26
	29C				19.47	81.40
	25C		lots of eggs, few larvae	normal	3.39	100.35
	25C				14.47	163.18
	25C				3.31	68.40
armi	29C	SH00116.N	no egg	intermediate	23.18	82.35
	29C				19.42	85.69
	29C				17.84	77.66
	25C		no egg	intermediate	63.41	206.39
	25C				41.90	170.65
piwi	29C	SH00477.N	no egg	tiny	5.33	10.61
	29C				9.15	35.90
	29C				3.63	6.85
	25C		no egg	tiny	7.47	23.47
	25C				8.23	20.80
	29C	SH00951.N	no egg	tiny	6.26	8.94
	29C				6.29	9.71
	25C		no egg	tiny	11.34	17.84
	25C				10.41	21.73
tudor	29C	SH00601.N	lots of eggs and larvae	normal	1.24	2.42
	29C				1.34	1.35
	25C		lots of eggs and larvae	normal	1.36	1.40
	25C				1.15	1.41
	25C				1.11	1.51

ShRNA females were crossed to *MTD-Gal4* males at the indicated temperature, and the resulting F1 females were crossed to wildtype (Ore^R) males to determine fertility. Total RNAs from ovaries were prepared and subjected to qRT-PCR analysis to determine the knockdown efficiency and degree of transposon de-repression. Results were first normalized against *rp49* levels and then to control samples from the *shRNA-w* cross.

Supplementary Table 2: ShRNA lines targeting genes that are not required for viability.

Nature Methods: doi.10.1038/nmeth.1592

Gene Name	Line Name	Crossed elav-Gal4		Crossed elav-Gal4/Cyo		Crossed Scratch-Gal4		Crossed RH1-Gal4		Crossed GMR-Gal4	
		25℃	29℃	25℃	29℃	25℃	29℃	25℃	29℃	25℃	29℃
w	SH000017	viable,white eye	viable,white eye	viable	viable	viable	viable	viable	viable		
TrpA1	SH000019	viable	viable	viable	viable	viable	viable	viable	viable	viable	viable
channel	SH000022	viable,male lethal	viable,male lethal	viable,male lethal	viable,male lethal	viable,male lethal	viable,male lethal	viable	viable	viable	viable
eye	SH000029	viable,eye-like O.N.	viable,eye-like O.N.	viable,eye-like O.N.	viable,eye-like O.N.	viable,eye-like O.N.	viable,eye-like O.N.	viable	viable	viable	viable
Galpha498	SH000032	lethal	lethal	lethal	lethal	lethal	lethal	viable	viable	viable	viable
InaC	SH000036	viable	viable	viable	viable	viable	viable	viable	viable	viable	viable
Arr2	SH000037	viable	viable	viable	viable	viable	viable	viable	viable	viable	viable
sev	SH000039	viable,sev-like O.N.	viable,sev-like O.N.	viable	viable	viable	viable	viable	viable	viable	viable

O.N. = optical neutralization

We generated shRNA lines against a number of genes for which null alleles are homozygous viable. Details on these genes and their associated phenotypes, as well as the used Gal4 lines, can be found in Ni et al.[1]. Data are courtesy of Robert Hardy and Charles Zuker.

Nature Methods: doi.10.1038/nmeth.1592

Supplementary Table 3: Transgenic long-hairpin RNAi lines analyzed for oogenesis phenotypes.

CG#	Gene name	Vector	TRiP#	Others
CG15793	Dsor1	VALIUM1	JF01697	
CG32443	Pc	VALIUM1	JF01581	
CG3954	csw	VALIUM1	HM04072	
CG4006	Akt1	VALIUM1	HM04007	
CG4257	Stat92E	VALIUM1	JF01265	
CG10079	Egfr	VALIUM10	JF01368	
CG12072	wts	VALIUM10	JF02741	
CG31666	chinmo	VALIUM10	JF02341	
CG3936	N	VALIUM10	JF01637	
CG4059	ftz-f1	VALIUM10	JF02738	
CG5671	Pten	VALIUM10	JF01987	
CG6667	dl	VALIUM10	JF02825	
CG7935	msk	VALIUM10	JF02727	
CG9885	dpp	VALIUM10	JF01371	
CG10023	Fak56D	VALIUM12	JF01646	
CG10595	d	VALIUM12	JF01668	
CG10917	fj	VALIUM12	JF01667	
CG11326	Tsp	VALIUM12	JF01644	
CG13345	tum	VALIUM12	JF01753	
CG13852	mats	VALIUM12	JF01690	
CG1389	tor	VALIUM12	JF01548	
CG14228	Mer	VALIUM12	JF01688	
CG14992	Ack	VALIUM12	JF01718	
CG1560	mys	VALIUM12	JF01645	
CG1730	dlg1	VALIUM12	JF01638	
CG17593	CG17593	VALIUM12	JF01903	
CG2019	disp	VALIUM12	JF01662	
CG2047	ftz	VALIUM12	JF01550	
CG2747	CG2747	VALIUM12	JF01643	
CG2759	w	VALIUM12	JF01543	
CG2759	w	VALIUM12	JF01546	
CG31094	LpR1	VALIUM12	JF01670	
CG3218	fs(1)K10	VALIUM12	JF01676	
CG32702	CG32702	VALIUM12	JF01663	
CG33193	sav	VALIUM12	JF01778	
CG3340	Kr	VALIUM12	JF01789	
CG3352	ft	VALIUM12	JF01689	
CG33991	nuf	VALIUM12	JF01642	
CG3936	N	VALIUM12	JF01575	
CG3969	PR2	VALIUM12	JF01647	
CG4005	yki	VALIUM12	JF01666	
CG4114	ex	VALIUM12	JF01687	
CG4656	Rassf	VALIUM12	JF01665	
CG6667	dl	VALIUM12	JF01862	
CG6716	prd	VALIUM12	JF01791	
CG6757	SH3PX1	VALIUM12	JF01760	
CG7793	Sos	VALIUM12	JF01555	
CG7935	msk	VALIUM12	JF02079	
CG8425	Jhe	VALIUM12	JF01669	
CG9885	dpp	VALIUM12	JF01372	
CG10260	CG10260	VALIUMp	JF01177	
CG10574	l-2	VALIUMp	JF01168	
CG14895	Pak3	VALIUMp	JF01175	
CG15305	flw	VALIUMp	JF01170	
CG31049	Doa	VALIUMp	JF01174	
CG4032	Abl	VALIUMp	JF01178	
CG5483	Lrrk	VALIUMp	JF01180	
CG6593	Pp1a-96A	VALIUMp	JF01171	
CG9115	mtm	VALIUMp	JF01115	
CG9156	Pp1-13C	VALIUMp	JF01169	
CG4006	Akt	pGD267		VDRC2902
CG1389	torso	pGD267		VDRC4298
CG3936	Notch	pGD267		VDRC27229
CG3218	K10	pGD267		VDRC102101
CG4257	Stat92E	pGD267		VDRC43866
CG3936	Notch	pUAST-R57		NIG3936R-2
CG4006	Akt	pUAST-R57		NIG4006R-1

Experiments were performed at both 25°C and 29°C. None of the lines tested showed oogenesis or embryonic phenotypes. VDRC and NIG lines correspond to lines obtained from the Vienna and National Institute of Genetics stock centers (http://stockcenter.vdrc.at/; http://www.shigen.nig.ac.jp/fly/nigfly), respectively.

Nature Methods: doi.10.1038/nmeth.1592

SUPPLEMENTARY NOTE 1:

RNAi via expression of long hairpins is not effective in the female germline

Previously, we reported the construction of long hairpin-based vectors, the "VALIUM series", and described in particular VALIUM1 and VALIUM10, that proved effective for RNAi in the soma[1,2] (**Supplementary Fig. 1a**). Both vectors contain *vermilion* as a selectable marker[3], an attB sequence to allow for targeted phiC31-mediated integration at genomic attP landing sites[4,5], two pentamers of UAS (one of which can be excised using the Cre/loxP system)[6] to generate a 5XUAS derivative for reduced expression levels[2]), the *hsp70* core promoter and a SV40 polyadenylation signal. An intronic sequence was placed between the two arms of the hairpin to facilitate hairpin RNA processing and nuclear export. A major difference between VALIUM1 and VALIUM10 is that the latter contains two gypsy insulator sequences to enhance transgene transcription[1]. Further differences concern the hairpin cloning strategy (multiple cloning site (MCS)-based for VALIUM1; recombination-based for VALIUM10) and an additional *ftz* intron upstream of the SV40 polyadenylation signal in VALIUM10. To test whether these vectors can drive transgene expression in the female germline, we used the *MTD-Gal4* line containing three different Gal4 insertions that drive expression at all stages of oogenesis[7] (see **Online Methods**). Although *MTD-Gal4* was able to drive expression of either *Luciferase* or *GFP* in a VALIUM1 and VALIUM10 vector (**Supplementary Figs. 1b,c**; data not shown for VALIUM1), we did not detect any germline or embryonic phenotypes when a number of long-hairpin transgenes were tested against genes associated with either oogenesis or maternal effect mutant phenotypes (data not shown; **Supplementary Table 3**). Our results extend a previous report showing that exogenously introduced long dsRNAs are ineffective in silencing target genes at certain stages of oogenesis[8].

To address the possibility that long-hairpin precursor transcripts were unstable in the germline, we added the 3'UTR of the maternally expressed *fs(1)K10* gene to VALIUM1 and VALIUM10[9] to generate VALIUM11 and VALIUM12. Both vectors carry the K10 3'UTR but differ in the presence or absence of the *ftz* 3'UTR intron (**Supplementary Fig. 1a**). Although this led to an overall increase in transgene expression, as determined by assaying a *Luciferase* marker (**Supplementary Fig. 1b**), it did not result in detectable germline or maternal effect phenotypes (data not shown; **Supplementary Table 3**). VALIUM11 and VALIUM12 were also much less effective at generating somatic RNAi phenotypes than VALIUM10, most likely because of the K10 3'UTR sequence (**Supplementary Fig. 7a,b**; data not shown for VALIUM11).

As VALIUM vectors possess the *hsp70* basal promoter that may not be optimal for germline expression[9], we tested a modified vector (VALIUMp) that contains both, the K10 3'UTR and the P-element transposase minimal promoter, which has been previously shown to efficiently drive expression in the female germline[9] (**Supplementary Fig. 1a**). VALIUMp was considerably more effective at driving either *Luciferase* or *GFP* in the germline (**Supplementary Fig. 1b,c**); however, the increased expression capacity did still not result in detectable phenotypes when long-hairpin constructs were expressed with *MTD-Gal4* (data not shown; **Supplementary Table 3**). As a final test of whether long dsRNAs could generate phenotypes in the female germline, we tested other commonly used vectors for somatic RNAi[10] (http://stockcenter.vdrc.at/control/main) (data not shown; **Supplementary Table 3**). As was observed with the VALIUM vectors, no phenotypes resulted from the expression of these long-hairpin constructs. Considered together, these results indicate that long dsRNAs are ineffective silencing triggers in female germ cells, even when delivered from vectors that can drive efficient expression of protein coding mRNAs.

Nature Methods: doi.10.1038/nmeth.1592

VALIUM20 is an effective vector for RNAi in both the female germline and the soma

Ovaries of *MTD-GAL4/UAS-shRNA-otu* or *MTD-GAL4/UAS-shRNA-bam* females showed ovarian tumor phenotypes that were morphologically identical to those associated with mutations in these genes (**Fig. 1b**). These phenotypes were fully penetrant at both 25°C and 29°C. The function of *otu* and *bam* is required in the germarium, indicating that VALIUM20 can effectively trigger RNAi during early oogenesis stages. VALIUM20 also proved effective at inducing RNAi at later stages. ShRNAs targeting *dl, tor* or *csw* led to the expected embryonic cuticle phenotypes (**Fig. 1c**). Depending on the shRNAs tested, the embryonic phenotypes were more severe when females with *MTD-Gal4* driven shRNAs were grown at 29°C rather than 25°C. For example, while *shRNA-dl* was fully penetrant both at 25°C and 29°C, approximately 5% of the embryos derived from *MTD-GAL4/UAS-shRNA-tor* hatched at 25°C but none hatched at 29°C. In the case of *shRNA-csw,* ~20% of the embryos hatched at 25°C while only ~2% hatched at 29°C. We also noticed that maternal age influenced phenotypic penetrance; eggs laid in the first 2-3 days following eclosion usually showed less penetrant phenotypes (data not shown).

To determine whether maternally loaded shRNAs can effectively knock down genes that are expressed zygotically, we generated shRNAs against a number of genes that result in embryonic lethality when mutated. For example, *decapentaplegic* (*dpp*) is expressed zygotically soon after fertilization and *dpp* mutant embryos show an almost complete replacement of the dorsal abdominal cuticle by ventral abdominal epidermal pattern elements[11]. This phenotype is solely dependent of the lack of zygotic *dpp* expression since the gene is not expressed in the female germline. Embryos derived from *MTD-GAL4/UAS-shRNA-dpp* mothers showed the characteristic *dpp* ventralization phenotype (**Fig. 1c**) demonstrating that maternally loaded shRNAs are effective at silencing mRNAs that are being transcribed following fertilization. As observed for other shRNAs, the phenotype was fully penetrant at 29°C but slightly weaker at 25°C.

Notch (*N*) is required for neurogenesis in early embryos. In the absence of zygotic *N*, embryos lack ventral cuticle due to hyperplasia of the nervous system[12]. In addition, *N* also has a maternal effect phenotype, as *N/+* embryos derived from *N* homozygous germline clones have a weak neurogenic phenotype. The neurogenic phenotype was observed in embryos derived from *MTD-GAL4/UAS-shRNA-N* females (**Fig. 1c**). Interestingly, *MTD-Gal4/UAS-shRNA-N* females could only be generated when *MTD-Gal4* males were crossed to *UAS-shRNA-N* females. Almost all *MTD-Gal4/UAS-shRNA-N* animals derived from *MTD-Gal4* females crossed to *UAS-shRNA-N* males died as embryos and showed a neurogenic phenotype or early larval stage lethality (data not shown). This strongly suggests an ability of maternally produced Gal4 to drive robust expression in the embryo of *UAS-shRNA-N* to levels sufficient to silence *N* transcripts. The neurogenic phenotype observed in embryos derived from *MTD-Gal4/UAS-shRNA-N* females was influenced by both temperature and maternal age. At 29°C the phenotype was 100% penetrant with all the embryos exhibiting a strong neurogenic phenotype. At 25°C, we observed a small fraction of hatching embryos during the first two days of egg laying (**Supplementary Fig. 8**). This age dependence may be caused by the first eggs made by females being produced faster than in older females[13], leading to a lower overall production and loading of maternal shRNAs.

We used *shRNA-N* and an shRNA against *white* (*shRNA-w)* to test the efficacy of VALIUM20 as a vector for RNAi in the soma. *UAS-shRNA-N*, in combination with the wing

Nature Methods: doi.10.1038/nmeth.1592

specific *C96-Gal4* driver, gave the wing phenotype that had been previously described[1,2] (**Fig. 1d**; data not shown). Notably, the phenotype was stronger than was previously achieved using a long hairpin in the optimized VALIUM10 vector (**Supplementary Fig. 3**). Similarly, when the *UAS-shRNA-w* line was tested with the eye specific *GMR-Gal4* driver, it generated an eye color phenotype similar to a complete null *white* mutation. This phenotype was again more severe than those generated previously using long dsRNA hairpins (**Fig. 1e**). To date, hundreds of shRNAs have been tested in the soma, and more than 90% generated the expected phenotypes (data not shown). Our combined results indicate that the expression of shRNAs from the VALIUM20 vector generates effective knockdown phenotypes in both the germline and the soma.

VALIUM22 is a superior vector for the female germline

In addition to the VALIUM22 experiments on silencing of piRNA pathway genes presented in **Fig. 2**, we tested the identical shRNAs expressed from the VALIUM20 vector. Very similar results were obtained upon depletion of Spn-E, Armi or Piwi using *MTD-Gal4* (**Supplementary Table 1**). Importantly, however, ovaries from flies expressing the *armi* or *piwi* shRNAs from VALIUM20 were rudimentary and resembled the phenotype of ovaries mutant for *piwi* or *armi* in germline and soma. This phenotype is highly suggestive of a significant depletion of Piwi or Armi in somatic support cells as *piwi* or *armi* are required in these cells for proper germline development[14,15]. We note that the identical shRNA sequences were used to generate the VALIUM20 and VALIUM22 constructs and that the identical genomic landing site was employed for the transgenes. Further, an independent shRNA expressed from VALIUM20 targeting a different region in *piwi* gave results identical to the previous *piwi* shRNA transgene. As homozygous *shRNA-piwi* or *shRNA-armi* lines are fertile, we speculate that low levels of Gal4 expression in the soma from *MTD-Gal4* trigger sufficient shRNA expression from VALIUM20 but not from VALIUM22 constructs. In support of this, shRNAs could be detected in carcasses (flies where the gonads were manually removed) when expressed from VALIUM20 using *MTD-Gal4* (**Supplementary Fig. 4**). Very low levels of processed shRNAs could even be detected in RNA samples prepared from the parental VALIUM20 shRNA fly stocks (**Supplementary Fig. 4**). We suspect that a temperature-sensitive element in the *hsp70* minimal promoter utilized in VALIUM20 allows for low-level expression that in combination with basal Gal4 levels leads to shRNA expression sufficient for gene knockdowns, at least in some cases. In summary, our results indicate that VALIUM22 is optimized for gene knockdowns and tissue specificity in the female germline, whereas VALIUM20 is favorable for silencing in somatic tissues.

Biogenesis and loading of shRNAs into effector complexes

To understand the genetic requirements of shRNA processing and loading, we depleted cultured *Drosophila* cells (Schneider/S2 cells) of components of the miRNA (Drosha, Pasha, Dcr-1, Loqs and AGO1) and siRNA (Dcr-2, Loqs, R2D2 and AGO2) pathways[16]. We compared the effects on shRNAs with those on a endogenous microRNA, *miR-bantam*, and the endogenous siRNA, *esi-2.1*. Knockdown of Drosha and Pasha simultaneously or depletion of Dcr-1 and AGO1 individually caused a significant reduction in levels of mature *miR-bantam* (**Supplementary Fig. 5a**). Depletion of Dcr-1 or Loqs caused a concomitant accumulation of the precursor miRNAs, whereas depletion of Dcr-2, R2D2 or AGO2 had no effect on levels of either precursor or mature *miR-bantam*. In contrast, depletion of Dcr-2, Loqs or AGO2 led to a

Nature Methods: doi.10.1038/nmeth.1592

substantial decrease of *esi-2.1* levels[16]. As expected due to their modeling onto an endogenous miRNA backbone, shRNAs behaved similar to *miR-bantam* with respect to knockdown of Drosha, Pasha, and Dcr-1 (effects of Loqs were too weak to reach a meaningful conclusion).

AGO1 and AGO2 both accept small RNAs from dsRNA precursors. However, they differ in their biochemical properties and in their bound populations of endogenous RNAs[17,18,19,20,21]. In addition, small RNAs that join AGO2 are modified at their 3' ends by the methyltransferase Hen1, making them resistant to β-elimination[22,23], which can be illustrated by the differential sensitivity of *esi-2.1*, which is AGO2-bound, and *miR-bantam*, which occupies AGO1. A substantial fraction of mature shRNAs resists β-elimination but becomes susceptible after depletion of AGO2 (**Supplementary Fig. 5a**). This suggests that AGO2 serves as the destination for the majority of shRNA strands. Support for this conclusion came from examination of AGO1 and AGO2 complexes (**Supplementary Fig. 5b**), although a substantial portion of shRNAs were also detected in AGO1 immunoprecipitates. Thus, although shRNAs are produced by the microRNA biogenesis machinery, they are efficiently loaded into AGO2, presumably by the canonical siRNA loading machinery consisting of Dcr-2 and R2D2. This is consistent with several recent reports of hierarchical loading rules for small RNAs in *Drosophila*, which predict that many of the shRNAs analyzed should show a preference for AGO2[17,18,19,20,21].

Abundance of shRNAs and processing accuracy

To reliably suppress their intended targets, shRNAs must be precisely and efficiently processed from their artificial precursor transcripts. In particular, the 5' end, a major determinant of target recognition via small RNAs must be predictable, so that design algorithms can aid in choosing potent shRNAs. While modeling on the *miR-1* backbone created some expectations of specific processing sites, this had to be tested explicitly in the remodeled constructs. We therefore transfected a number of different shRNA constructs into cultured S2 cells and sequenced the small RNA populations from these cells. The vast majority of shRNAs in these libraries generated from total RNAs (19- to 24-nt) were 22-nt in size (**Supplementary Fig. 6a**). Importantly, the guide shRNA strands derived from the 3p arm of the hairpin and their respective 5' ends precisely corresponded to the expected products, indicating accurate Dcr-1 cleavage. The 3' ends of shRNAs show slight variation, similar in extent to endogenous miRNAs. Furthermore, guide shRNA strands derived from the 3p arm were invariably higher in abundance than their passenger counterparts from the 5p arm (**Supplementary Fig. 6a,b**). In order to evaluate cellular shRNA levels, we compared their abundances and strand biases with those of the 30 most abundant endogenous miRNAs from three independent transfections. We found shRNA guide strand levels comparable to those of highly abundant microRNAs (**Supplementary Fig. 6b**), while their passenger strands ranked similarly to miR* strands. Also, strand selection of shRNAs parallels that of most miRNAs with strong biases towards the guide/miR strands (**Supplementary Fig. 6b**). Considered together, these data indicate that placing a sequence perfectly complementary to the target of interest into the 3p arm of the *miR-1* backbone (together with a suitable 5p arm sequence) leads to efficient and accurate production of the intended small RNA.

Nature Methods: doi.10.1038/nmeth.1592

SUPPLEMENTARY NOTE 2: Vector construction

VALIUM11 and VALIUM12: To construct VALIUM11, the *SV40* polyA signal of *VALIUM10*[1] was replaced with fill-in nucleotides (fwd: 5'-AATTGAACCGCGGAATCGATTCTGCAGTTGAGCT-3', rev: 5'-CAACTGCAGAATCGATTCCGCGGTTC-3') using SacI and SacII. The vector was then cut with MfeI and PstI, and filled with a 1.7kb *K10* 3'UTR from *UASp*[9]. To construct VALIUM12, the *ftz* intron was amplified with specific primers (fwd: 5'-CCTCTAGAGAATTGTTGGCATCAGGTAGG-3', rev: 5'-TTCAATTGCCGCGGCTCTAGTTCTTTG-3') from VALIUM1[2]. The PCR product was cut with XbaI and MfeI, and then cloned into VALIUM11.

VALIUMp: The *SV40* polyA signal of VALIUM1 w*as* replaced with fill-in nucleotides (fwd: 5'-AATTGAACCGCGGAATCGATTCTGCAGTTGAGCT-3', rev: 5'-CAACTGCAGAATCGATTCCGCGGTTC-3') using SacI and MfeI. The resulting vector was cut with MfeI and PstI, and a 1.7kb *K10* 3'UTR was inserted. The P-element transposase promoter from *UASp* was amplified (fwd: 5'-TCGTCGACAGCCGTAGCTTACCGAAGTATAC-3', rev: 5'-CTGAATTCTGATCCCCGGGCGGGTACCA-3'), the PCR product was cut with SalI and EcoRI, and then cloned into the previous vector.

Luciferase and GFP constructs: To generate the *Luciferase* and *GFP* VALIUM constructs, VALIUM1-*Luciferase* and VALIUM1-*GFP*[1] were cut with EcoRI and XbaI. A 1.8kb DNA fragment containing the *Luciferase* coding region and the small fragment carrying *GFP* were gel purified, and subsequently cloned into VALIUM10, VALIUM11, VALIUM12 and VALIUMp using the same restriction sites. For the *Luciferase* assay, ovaries were dissected in 1XPBS and pooled into groups of 5 in 50 uL Glo Lysis Buffer (Promega). Ovaries were stored frozen at -80^{o}C until further use. Following thawing and homogenizing with an eppendorf pestle, *Luciferase* readings were measured using the Steady Glo Luciferase Assay System (Promega).

VALIUM20: To construct VALIUM20, VALIUM10 was cut with EcoRI and XbaI resulting in five fragments. The largest fragment was gel purified and ligated with an oligonucleotide fragment generated by annealing the two primers (fwd: 5'-AATTGAGATCTGTTGTAGAGTGGACATATGCACCTAGGA-3', rev: 5'-CTAGTCCTAGGTGCATATGTCCACTCTACAACAGATCTC-3'), this resulted in an intermediate vector. pNE3 (gift from Benjamin Haley) was cut with XbaI and NdeI which produced two fragments. The small fragment was gel purified and cloned into the aforementioned intermediate vector that was linearized with XbaI and NdeI.

VALIUM22: To construct VALIUM22, VALIUM2[1] was cut with EcoRI and BamHI. The fragment containing the *P*-element transposase promoter was cloned into pre-linearized VALIUM12. A DNA fragment containing the *miR-1* scaffold was obtained by PCR (fwd: 5'-AATTGAGATCTGTTGTAGAGTG-3', rev: 5'-CTAGGTGCATATGTCCACTCT-3'), and then cloned into the previous vector, which was cut with EcoRI and XbaI, to yield VALIUM22.

shRNA construct: The following steps were used to design and construct the shRNAs:

1. Selection of the 21-nt sequence based on the algorithm of Vert et al.[24];

2. The oligonucleotide design eliminates off target effect at 16nt;

3. Based on *miR-1* scaffold, for the top strand oligo, add ctagcagt to 5' end of passenger strand DNA, add tagttatattcaagcata between passenger strand DNA and guide strand DNA, add gcg to 3' end of guide strand DNA, so the resulting oligo will be:

Nature Methods: doi.10.1038/nmeth.1592

5’-ctagcagtNNNNNNNNNNNNNNNNNNNNNtagttatattcaagcataNNNNNNNNNNNNNNNNNNNNgcg-3’;

4. For the bottom strand oligo, add aattcgc to 5’ end of guide strand DNA, add tatgcttgaatataacta between guide strand DNA and passenger strand DNA, add actg to 3’ end of passenger strand DNA, so the resulting oligo will be:

5’-aattcgcNNNNNNNNNNNNNNNNNNNNNtatgcttgaatataactaNNNNNN NNNNNNNNNNNNNNactg-3’;

5. Annealing top strand with bottom strand oligos, the resulting DNA fragment has overhangs for NheI and EcoRI;

6. Directly clone this DNA fragment into VALIUM20 vector that had been linearized by NheI and EcoRI. Bacteria string TOP10 cells were used as competent cells;

7. PCR select correct clone, and the primers we used are:

fwd: 5'-ACCAGCAACCAAGTAAATCAAC-3'

rev: 5'-TAATCGTGTGTGATGCCTACC-3';

8. DNA sequencing to confirm correct shRNA construct, and the sequencing primer is: 5’-ACCAGCAACCAAGTAAATCAAC-3’.

Nature Methods: doi.10.1038/nmeth.1592

SUPPLEMENTARY NOTE 3: Primer sequences

Northern Blotting: The sequences of the oligonucleotide probes are:

esi-2.1	5'-GGAGCGAACTTGTTGGAGTCAA-3'
miR-bantam	5'-AATCAGCTTTCAAAATGATCTCA-3'
2S rRNA	5'-TACAACCCTCAACCATATGTAGTCCAAGCA-3'
shRNA-E(bx)	5'-CAGCTTGTGGTTCAACAACAA-3'
shRNA-N	5'-CGCGGCGGTTAACAATACCGAA-3'

Transposon qPCR analysis: The sequences of the oligonucleotides used are:

nos-fwd:	5'-GCAACTTAATGCCCATTCCAC-3'
nos-rev:	5'-CGGCTGGTATATACGACATGT-3'
rp49-fwd:	5'-CCGCTTCAAGGGACAGTATCTG-3'
rp49-rev:	5'-ATCTCGCCGCAGTAAACGC-3'
HeT-A-fwd:	5'-CGCCGCAGTCGTTTGGTGAGT-3'
HeT-A-rev:	5'-CGCGCGGAACCCATCTTCAGA-3'
blood-fwd:	5'-CCAACAAAGAGGCAAGACcG-3'
blood-rev:	5'-TCGAGCTGCTTACGCATACTGTC-3'

Nature Methods: doi.10.1038/nmeth.1592

REFERENCES:

1. Ni, J. Q. *et al.*, *Genetics* **182**, 1089-1100 (2009).
2. Ni, J. Q. *et al.*, *Nat Methods* **5**, 49-51 (2008).
3. Fridell, Y. W. and Searles, L. L., *Nucleic Acids Res* **19**, 5082 (1991).
4. Thomason, L. C., Calendar, R., and Ow, D. W., *Mol Genet Genomics* **265**, 1031-1038 (2001).
5. Groth, A. C., Fish, M., Nusse, R., and Calos, M. P., *Genetics* **166**, 1775-1782 (2004).
6. Siegal, M. L. and Hartl, D. L., *Genetics* **144**, 715-726 (1996).
7. Petrella, L. N., Smith-Leiker, T., and Cooley, L., *Development* **134**, 703-712 (2007).
8. Kennerdell, J. R., Yamaguchi, S., and Carthew, R. W., *Genes Dev* **16**, 1884-1889 (2002).
9. Rorth, P., *Mech Dev* **78**, 113-118 (1998).
10. Dietzl, G. *et al.*, *Nature* **448**, 151-156 (2007).
11. Irish, V. F. and Gelbart, W. M., *Genes Dev* **1**, 868-879 (1987).
12. Jiménez, F., Campos-Ortega, J. A. , *Wilhelm Roux's Archives* **191** (1982).
13. King, R. C., *Ovarian Development in Drosophila melanogaster.* . (Academic Press, New York. , 1970).
14. Cook, H. A., Koppetsch, B. S., Wu, J., and Theurkauf, W. E., *Cell* **116**, 817-829 (2004).
15. Cox, D. N. *et al.*, *Genes Dev* **12**, 3715-3727 (1998).
16. Czech, B. *et al.*, *Nature* **453**, 798-802 (2008).
17. Tomari, Y., Du, T., and Zamore, P. D., *Cell* **130**, 299-308 (2007).
18. Forstemann, K. *et al.*, *Cell* **130**, 287-297 (2007).
19. Okamura, K., Liu, N., and Lai, E. C., *Mol Cell* **36**, 431-444 (2009).
20. Czech, B. *et al.*, *Mol Cell* **36**, 445-456 (2009).
21. Ghildiyal, M. *et al.*, *RNA* **16**, 43-56 (2010).
22. Horwich, M. D. *et al.*, *Curr Biol* **17**, 1265-1272 (2007).
23. Saito, K. *et al.*, *Genes Dev* **21**, 1603-1608 (2007).
24. Vert, J. P., Foveau, N., Lajaunie, C., and Vandenbrouck, Y., *BMC Bioinformatics* **7**, 520 (2006).

Nature Methods: doi.10.1038/nmeth.1592

Nature Methods: doi.10.1038/nmeth.1592